Available online at www.sciencedirect.com
SCIENCE DIRECT®
Journal of Sound and Vibration 285 (2005) 281–302
JOURNAL OF SOUND AND VIBRATION
www.elsevier.com/locate/jsvi

A phenomenological model of active constrained layers

Hélène Illaire[a,*], Wolfgang Kropp[a], Brian Mace[b]

[a]*Department of Applied Acoustics, Chalmers University of Technology, 412 96 Göteborg, Sweden*
[b]*Institute of Sound and Vibration Research, University of Southampton, Southampton SO17 1BJ, UK*

Received 24 March 2004; accepted 23 August 2004
Available online 2 December 2004

Abstract

Active constrained layer (ACL) treatments consist of a layer of viscoelastic material bonded to the host structure and constrained by an actuator. These treatments control vibrations by means of several mechanisms: the actuator increases the dissipation of energy by increasing the shearing in the viscoelastic layer, and simultaneously it controls the vibrations by applying forces to the host structure through the viscoelastic layer. To optimise ACL treatments, it is necessary to understand their physics. While several models in the literature successfully predict the response of structures treated with ACL, the complexity of these models is not well suited for investigating the mechanisms underlying the behaviour of ACL treatments.

This paper describes a simple model of beams treated with ACL, which allows analytical investigations of the damping and control mechanisms of ACL treatment. The model is based on a modal approach in which each mode of the structure is represented by a mass–spring system. The two layers of the ACL patch are represented by two springs in series, the control voltage in effect driving one of these springs. A numerical validation indicates that the model accuracy is good for ACL patches whose length is smaller than the wavelength of the beam and located at appropriate positions on the host structure.

In order to demonstrate the usefulness of the lumped parameter model to get insight into the behaviour of ACL treatments, the various ACL damping mechanisms are briefly discussed. Results indicate that proportional feedback control is associated with an increase of shearing in the viscoelastic layer, while the action of active forces dominates when derivative feedback is used.

*Corresponding author. Tel.: +46 31 772 2200; fax: +46 31 772 2212.
E-mail address: helene@ta.chalmers.se (H. Illaire).

0022-460X/$ - see front matter © 2004 Elsevier Ltd. All rights reserved.
doi:10.1016/j.jsv.2004.08.029

1. Introduction

An interesting technique to reduce vibrational energy is to use active control in conjunction with material damping, because active control is easier to implement at low frequencies while material damping is generally more efficient at high frequencies. Moreover, material damping adds stability to the system, potentially improving the efficiency of the active control. An example of active–passive treatment for structural vibrations is the active constrained layer (ACL). This treatment consists of a viscoelastic layer constrained by an actuator, generally made of piezoelectric material, and dissipates energy simultaneously by the shearing of the constrained viscoelastic layer and by the action of the actuator. In the typical configuration shown in Fig. 1, the viscoelastic layer is sandwiched between the structure and the piezoelectric actuator, across which a control voltage is applied. If the actuator is properly driven by the control voltage, it increases the shearing of the viscoelastic layer and the dissipation of energy. The actuator also applies forces to the host structure through the viscoelastic layer, further controlling the vibrations.

To optimise ACL treatments, it is essential to understand and model the physics underlying their behaviour. In the literature, a number of models of structures treated with ACL have been derived and validated by experiments. Several of these models are based on finite element analysis, for example, those proposed by Baz [1] or by Liao and Wang [2] for beams, and by Park and Baz [3] for plates. Rongong's model [4] using the Rayleigh–Ritz method was also validated experimentally. Analytical models have also been proposed. For example, Baz [5–7] and Shen [8,9] have used mechanics of material or energy approaches (such as Hamilton's principle) to obtain a sixth-order differential equation describing beams treated with ACL. In Baz' model, this equation has been solved using a wave approach [5,6]. Following the work of Baz, a similar model has been experimentally validated by Illaire and Kropp [10].

Although these models are useful as detailed prediction tools, they are not well suited to understanding the behaviour of ACL treatment, since the mathematical expressions involved are very complex. These models behave as ''black boxes'': they accurately predict the response of the structure, but they do not allow for the investigation of the underlying mechanisms in a direct, analytical way.

This paper describes a simple model of beams treated with ACL, which provides insight into the physics of ACL treatments. In this model, referred to here as the 'lumped parameter model', each mode of the base beam is modelled as a single degree of freedom (sdof) system, and the two layers of the ACL patch are modelled by two springs in series, as shown in Fig. 2. The spring modelling the actuator is driven by a modal force V_n resulting from the voltage V applied to this actuator.

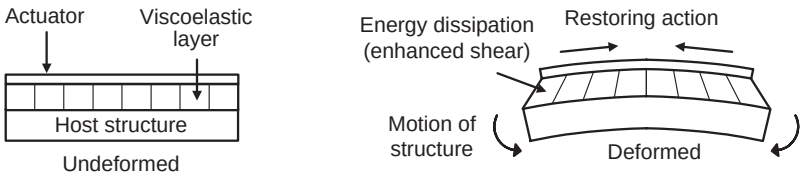

Fig. 1. Principle of active constrained layer.

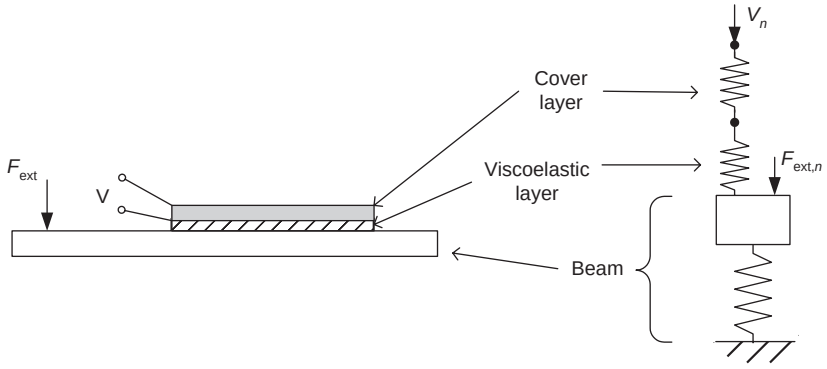

Fig. 2. Principle of the lumped parameter model.

The stiffness corresponding to the viscoelastic layer is complex, reflecting the dissipative nature of viscoelastic materials, while the stiffness corresponding to the actuator is approximated to be real.

The main assumption of the model is that the surface strain of the beam beneath the ACL patch is constant. Therefore, the model is valid for patches whose length is short compared to the wavelength on the beam and which are positioned around the antinodes of the beam.

The lumped parameter model enables analytical investigations and the interpretation to be made of issues such as the influence of the control law and of the viscoelastic layer characteristics on the dissipation of energy, or on the transmission of the active force to the host structure.

The variables describing the beam and the ACL patch modelled in this work are given in Section 2, and the assumptions made in the model are presented in Section 3. The equivalent spring stiffness of each layer of the uncoupled ACL patch are calculated in Section 4. The lumped parameter model is derived using a modal approach in Section 5, and is validated in Section 6 by comparing numerical predictions with those of a more detailed wave model [10]. In Section 7, the various effects of ACL treatments are explored.

2. Description of the structure

The structure modelled in this article is a beam treated with an ACL patch, as shown in Fig. 3. The geometrical and material characteristics of the structure are described by the following variables:

- L is the length of the beam, and L_a is the length of the ACL patch;
- x_1 and x_2 are the positions at the ends of the ACL patch, and x_c is the position of the center of the ACL patch;
- the width of the beam is b;
- t_b, t_v and t_c are the thicknesses of the base beam, viscoelastic layer and cover layer, respectively;
- the mass per unit length of the base beam is ρ;
- E_b and E_c are the Young's moduli of the base and cover layer;
- I_b is the moment of inertia of the base layer;

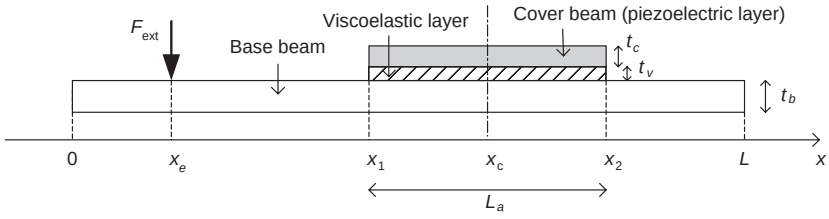

Fig. 3. Geometry of the beam with an ACL patch.

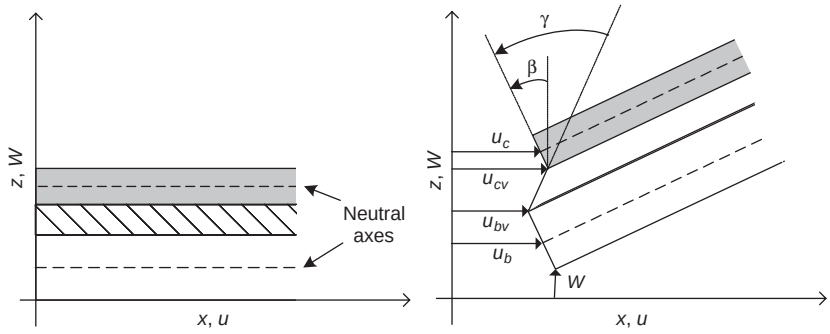

Fig. 4. Variables describing the motion of the structure.

- G is the complex shear modulus of the viscoelastic layer; $G = G'(1 + j\eta_G)$, where G' is the storage modulus and η_G the loss factor;
- d_{31} is the strain constant of the piezoelectric material of the cover layer.

The structure is subjected to a transverse external force $f_{ext}(t)$ at some position x_e, and to a control voltage $v(t)$ applied to the piezoelectric cover layer. It is assumed that the force and the voltage are time harmonic at frequency ω so that $f_{ext}(t) = F_{ext}e^{j\omega t}$ and $v(t) = Ve^{j\omega t}$. Thus, all dynamic quantities vary as $e^{j\omega t}$ and this explicit time dependance will be suppressed henceforth. The control voltage results in a free strain ε_p in the cover layer, given by

$$\varepsilon_p = V\frac{d_{31}}{t_c}. \tag{1}$$

These excitations cause bending motion in the structure, this motion is described by several variables (see Fig. 4):

- W is the transverse displacement of the layers;
- u_b and u_c are the longitudinal displacements of the base beam and of the cover layer, respectively;
- u_{bv} and u_{cv} are the longitudinal displacements of the viscoelastic layer at the interface with the base beam and with the cover layer, respectively;
- the shear strain in the viscoelastic layer is $\gamma = (u_{cv} - u_{bv})/t_v$;
- the extensional strain in the base and cover layer is $\varepsilon_b = \mathrm{d}u_b/\mathrm{d}x$ and $\varepsilon_c = \mathrm{d}u_c/\mathrm{d}x$, respectively;
- the bending angle of the structure is $\beta = \mathrm{d}W/\mathrm{d}x$.

The stress and the strain in the base layer, the viscoelastic layer and the cover layer, respectively, are related by the following equations:

$$\tau = G\gamma, \tag{2}$$

$$\sigma_c = E_c(\varepsilon_c - \varepsilon_p), \tag{3}$$

$$\sigma_b = E_b\varepsilon_b. \tag{4}$$

In addition, the extensions e_b and e_c of the viscoelastic layer at the interface with the beam and with the cover layer, respectively, are

$$e_b = L_a\varepsilon_b, \tag{5a}$$

$$e_c = L_a\varepsilon_c, \tag{5b}$$

and the extension e_p induced in the cover layer by the control voltage is

$$e_p = L_a\varepsilon_p, \tag{6}$$

where ε_p is the free strain as defined in Eq. (1).

3. Assumptions

The main assumption is that the strain of the surface of the beam is constant underneath the ACL patch. The conditions under which this assumption is valid depend on the size of the patch and its position on the beam with respect to the nth mode shape, and are considered in Section 3.1.

Other simplifying assumptions, valid for a thin ACL patch, are that the mass of the patch and the bending stiffness of the cover layer are negligible. Also, it is assumed that the ACL patch introduces negligible coupling between the modes of the uncontrolled beam.

Other assumptions in the model developed here are commonly made for models of structures treated with ACL (see e.g. Refs. [1–9]). These include:

- the classical Euler–Bernouilli assumptions apply for the base layer;
- the deflection in the direction normal to the surface is the same for all layers, i.e. there is no transverse compression in any of the layers;
- only shear motion takes place in the viscoelastic layer, and the shear angle is constant across the depth of the viscoelastic layer;
- only bending motion occurs in the base layer;
- the cover layer only extends or contracts;
- the electrical potential in the electrodes of the actuator is uniform, and electro-mechanical coupling effects are neglected.

3.1. Conditions for a constant surface strain of the beam

In the lumped parameter model, it is assumed for simplicity that the strain of the surface of the beam is constant underneath the ACL patch. In the following, we examine the conditions under which this condition is true.

In order to simplify the analysis, consider the case of a cover layer whose longitudinal stiffness is negligible compared to that of the base beam, i.e. $t_c E_c \ll t_b E_b$. In such a case, the base beam experiences a bending motion with negligible net axial extension. Then, the strain ε_{bv} at the surface of the beam can be approximated by

$$\varepsilon_{bv} = \frac{t_b}{2} \frac{\mathrm{d}^2 W}{\mathrm{d}x^2}. \tag{7}$$

Assuming vibrations in modes, around the nth natural frequency of the beam the transverse displacement is equal to the mode shape $\Phi_n(x)$ and therefore

$$\varepsilon_{bv}(x) = C_n \frac{\mathrm{d}^2 \Phi_n}{\mathrm{d}x^2}(x), \tag{8}$$

where C_n is the amplitude of the nth modal component of ε_{bv}. Expanding $\varepsilon_{bv}(x)$ as a Taylor series about the center of the ACL patch at $x = x_c$ gives

$$\varepsilon_{bv}(x_c) = C_n \left(\frac{\mathrm{d}^2 \Phi_n}{\mathrm{d}x^2}(x_c) + (x - x_c) \frac{\mathrm{d}^3 \Phi_n}{\mathrm{d}x^3}(x_c) - \frac{(x - x_c)^2}{2!} \frac{\mathrm{d}^4 \Phi_n}{\mathrm{d}x^4}(x_c) + \cdots \right). \tag{9}$$

The strain is thus constant with position if all terms of order higher than one in the equation above can be neglected. As an example, for a simply supported beam with an ACL patch of length L_a, the strain beneath the ACL patch is constant if

$$\frac{L_a}{2} k_n |\cot k_n x_c| \ll 1 \tag{10}$$

and

$$\frac{1}{2} \left(\frac{L_a}{2} k_n \right)^2 \ll 1. \tag{11}$$

Therefore, the strain is constant if the length of the ACL patch L_a is small enough (compared to the wavelength $2L/n$) and if the patch is mounted at an appropriate position x_c on the beam, such that $\sin k_n x_c$ is large enough. This latter condition is required for the patch to adequately couple into the nth mode of the beam.

As an illustrated example, if the patch is centered on an antinode of the beam, then Eq. (10) is always fulfilled and the maximum length of the patch is given by Eq. (11). It can easily be calculated that in this case, the deviation from linearity at the ends of each zone is equal to 10% if $L_a/L = 0.29/n$. For each mode, the maximum length of an ACL patch centered on an antinode of the beam is thus equal to about one-sixth of the wavelength of the beam.

4. Equivalent stiffness of an uncoupled ACL patch

In this section, we derive the equivalent stiffness of the springs modelling the viscoelastic layer and the cover layer of the ACL patch when it is uncoupled, i.e. not bonded to the host structure. First, the shear stress inside the viscoelastic layer is calculated when a known constant strain is applied at the base of the ACL patch. Second, an equivalent stiffness is derived for each layer.

This equivalent stiffness relates the applied shear force and the extensions of a layer, and will be used in Section 5 to derive the stiffness of the ACL patch coupled to the host structure.

4.1. Equation of motion of the ACL patch

An ACL patch of length L_a is subjected to an extensional strain of constant amplitude at its base, such that $\varepsilon_b = e_b/L_a$ (see Fig. 5). Therefore, the longitudinal displacement u_{bv} of the base of the viscoelastic layer, apart from a constant term, is given by

$$u_{bv}(y) = \frac{e_b}{L_a} y, \tag{12}$$

where $y = x - x_c$ is the position with respect to the centre of the patch.

Equilibrium of forces in the longitudinal direction yields

$$\frac{\mathrm{d}T_c}{\mathrm{d}y} - b\tau = 0, \tag{13}$$

where T_c is the axial force in the cover layer. In this equation, it is assumed that the inertial forces resulting from the axial displacement of the base and of the cover layer are negligible. Inserting Eqs. (2), (3) and (12) into Eq. (13) yields

$$\frac{\mathrm{d}^2 u_{cv}}{\mathrm{d}y^2} - g u_{cv} = -g \frac{e_b}{L_a} y, \tag{14}$$

where

$$g = \frac{G}{t_v} \frac{1}{t_c E_c}. \tag{15}$$

The parameter g is associated with the coupling between the base and the cover layer.

The particular solution of Eq. (14) is

$$u_{cv} = C_1 \mathrm{e}^{\sqrt{g}y} + C_2 \mathrm{e}^{-\sqrt{g}y} + \frac{e_b}{L_a} y \tag{16}$$

and is the sum of two evanescent components and of a component arising from the excitation. The constants C_1 and C_2 can be found from the boundary conditions at the ends of the cover layer. The axial force and hence the axial stress in the constraining layer is zero at the ends of the cover

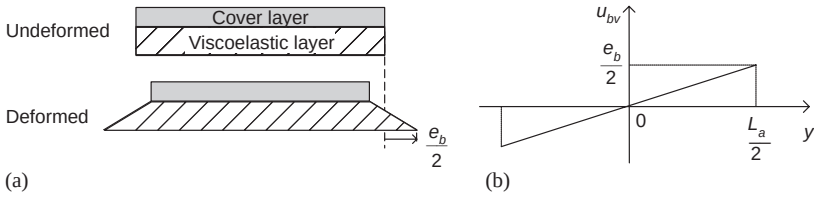

Fig. 5. ACL patch subjected to an extensional strain of constant amplitude: (a) deformation of the ACL patch and (b) applied longitudinal displacement at the base of the patch.

layer. Consequently,

$$\sigma_c\left(-\frac{L_a}{2}\right) = \sigma_c\left(\frac{L_a}{2}\right) = 0. \tag{17}$$

Thus, we obtain

$$C_1 = -C_2 = \frac{\varepsilon_p - (e_b/L_a)}{\sqrt{g}\,\cosh(\zeta)}, \tag{18}$$

where ζ is a non-dimensional parameter given by

$$\zeta = \sqrt{g}\frac{L_a}{2}. \tag{19}$$

This yields

$$u_{cv}(y) = \frac{\sinh(\sqrt{g}y)}{\sqrt{g}\,\cosh(\zeta)}\left(\varepsilon_p - \frac{e_b}{L_a}\right) + \frac{e_b}{L_a}y. \tag{20}$$

The shear stress $\tau(y)$ can be deduced from Eq. (2), and is given by

$$\tau(y) = \frac{2E_c t_c}{L_a^2}\frac{\zeta}{\cosh(\zeta)}\sinh(\sqrt{g}y)(e_p - e_b). \tag{21}$$

The term $e_p = L_a\varepsilon_p$ is the extension that would be induced by the control voltage in the cover layer if this layer was free, i.e. not bonded to the viscoelastic layer. The amplitude of $\tau(y)$ depends thus on the extensions e_p and e_b of the top and the base of the ACL patch.

The term $\sinh(\sqrt{g}y) = \mathrm{e}^{\sqrt{g}y} - \mathrm{e}^{-\sqrt{g}y}/2$ represents end effects whose relative importance increases with ζ. As shown in Fig. 6, the variation of the function $\tau(y)$ is nearly linear for small values of ζ and tends to $\delta(y - L_a/2) + \delta(y + L_a/2)$, where δ is the Dirac function, for large values of ζ. This last case corresponds to an ACL patch whose viscoelastic layer is very thin and stiff compared to the cover layer ($t_v/G \ll E_c t_c$), i.e. to an actuator directly bonded to the host beam.

4.2. Equivalent stiffness of the viscoelastic layer

The shear stiffness κ_v of the viscoelastic layer alone, as shown in Fig. 7, is

$$\kappa_v = \frac{F_{\text{shear}}}{e_c - e_b}, \tag{22}$$

where F_{shear} is the shear force applied to the right half of the upper surface of the viscoelastic layer, i.e.

$$F_{\text{shear}} = b\int_0^{L_a/2}\tau(y)\,\mathrm{d}y. \tag{23}$$

To derive κ_v, it is necessary to calculate the shear stress function $\tau(y)$ as a function of e_c and e_v. Eq. (21) shows that $\tau(y)$ has the form

$$\tau(y) = A\,\sinh(\sqrt{g}y). \tag{24}$$

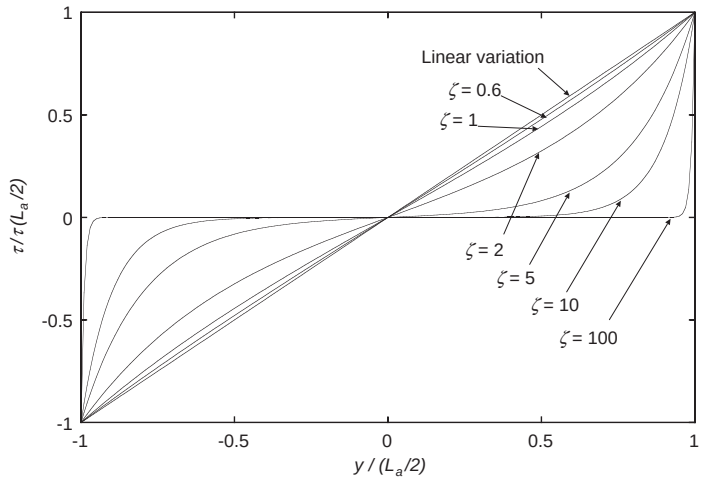

Fig. 6. Variation of the shear stress $\tau(y)$ for different values of ζ.

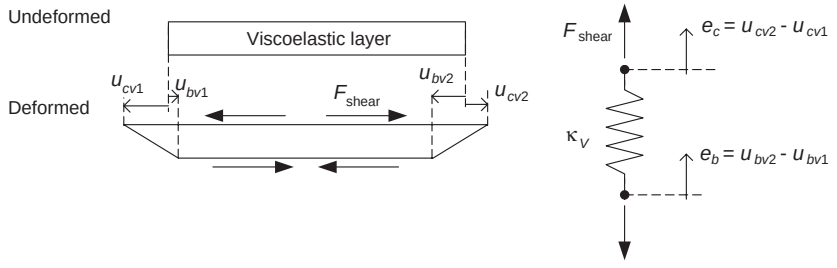

Fig. 7. Modelling of the viscoelastic layer as a spring.

The amplitude A has to satisfy the boundary conditions

$$\tau\left(\frac{L_a}{2}\right) = \frac{G}{t_v}(u_{cv2} - u_{bv2}), \tag{25}$$

$$\tau\left(-\frac{L_a}{2}\right) = \frac{G}{t_v}(u_{cv1} - u_{bv1}), \tag{26}$$

which yields

$$A = 2\,\frac{E_c t_c}{L_a^2}\,\frac{\zeta^2}{\sinh(\zeta)}\,(e_c - e_b). \tag{27}$$

Substituting Eqs. (24) and (27) into Eq. (23) leads to

$$\kappa_v = b\,\frac{E_c t_c}{L_a}\,\frac{\cosh(\zeta)-1}{\sinh(\zeta)/\zeta}. \tag{28}$$

If the viscoelastic layer is very stiff and thin in comparison with the cover layer, then ζ becomes very large. In this case, κ_v also becomes very large, meaning that the spring becomes very stiff. The cover layer is in effect then bonded directly to the host beam. If, on the other hand, the viscoelastic layer is soft and thick in comparison with the cover layer, ζ and κ_v tend to zero. In this case, the cover layer is effectively uncoupled from the host structure.

4.3. Equivalent stiffness of the cover layer

The equivalent stiffness κ_c of the cover layer as shown in Fig. 8 is

$$\kappa_c = \frac{F_{\text{shear}}}{e_p - e_c}. \tag{29}$$

To derive κ_c, we need first to calculate τ as a function of e_c and e_p. The shear stress τ on the upper surface of the viscoelastic layer and the extensional stress σ in the cover layer are related by

$$t_c\,\frac{\mathrm{d}\sigma}{\mathrm{d}y} = \tau \tag{30}$$

from equilibrium. Therefore, σ is given by

$$\sigma(y) = \frac{A}{t_c}\,\frac{1}{\sqrt{g}}\cosh(\sqrt{g}y) + C, \tag{31}$$

where C is a constant. Applying the boundary conditions (zero axial stress at the ends of the cover layer) leads to

$$C = -\frac{A}{t_c}\,\frac{\cosh(\zeta)}{\sqrt{g}}. \tag{32}$$

In addition, σ must satisfy the relation for the cover layer given in Eq. (3), and therefore

$$\frac{\mathrm{d}u_c}{\mathrm{d}y} = \frac{\sigma}{E_c} + \varepsilon_p. \tag{33}$$

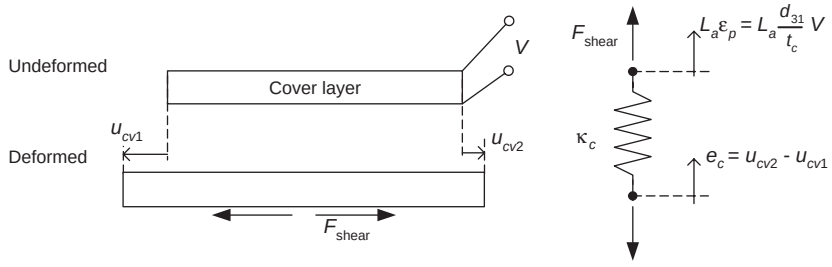

Fig. 8. Modelling of the cover layer as a spring.

Integrating this equation yields

$$u_c = \frac{1}{\sqrt{g}} \frac{A}{E_c t_c} \left(\frac{1}{\sqrt{g}} \sinh(\sqrt{y}) - y \cosh(\zeta) \right) + \varepsilon_p y + D. \tag{34}$$

Then, calculating $e_c = u_c(L_a/2) - u_c(-L_a/2)$ gives

$$A = \frac{E_c t_c g}{2 \sinh(\zeta) - 2\zeta \cosh(\zeta)} (e_c - e_p). \tag{35}$$

Inserting this expression in Eqs. (30) and (31) gives τ, and finally Eqs. (23) and (29) yield

$$\kappa_c = b \frac{E_c t_c}{L_a} \frac{\cosh(\zeta) - 1}{\cosh(\zeta) - \sinh(\zeta)/\zeta}. \tag{36}$$

If ζ tends to infinity, κ_c tends to $bE_c t_c/L_a$. This value corresponds to the stiffness of a beam subjected to a strain which is constant with position. When the strain in the cover layer is not constant, κ_c is larger than this limiting value.

4.4. Total equivalent stiffness of the ACL patch

The force applied by the ACL patch to the beam obeys

$$F_{\text{shear}} = \kappa_{\text{acl}}(e_b - e_p), \tag{37}$$

where κ_{acl} is the equivalent stiffness of the ACL patch and is equal to the stiffness of the viscoelastic layer and the cover layer in series, i.e.

$$\frac{1}{\kappa_{\text{acl}}} = \frac{1}{\kappa_v} + \frac{1}{\kappa_c}. \tag{38}$$

Inserting the expressions for κ_v and κ_c given in Eqs. (28) and (36) yields

$$\kappa_{\text{acl}} = b \frac{E_c t_c}{L_a} \frac{\cosh(\zeta) - 1}{\cosh(\zeta)}. \tag{39}$$

If κ_c is much smaller than κ_v, which happens when $\zeta \gg 1$, then $\kappa_{\text{acl}} = \kappa_c$ (see Fig. 9) and the cover layer can be considered to be directly bonded to the beam. The approach presented here thus enables to model ACL patches with arbitrarily thin and stiff viscoelastic layers. For low values of ζ, $\kappa_{\text{acl}} = \kappa_v$ and the cover layer can be considered to be perfectly rigid. In this case, the shear stress in the viscoelastic layer varies linearly with x. As will be seen in Section 7, the constrained layer is optimum for some intermediate value of ζ.

The equivalent stiffness κ_{acl} is an approximate lumped parameter model of the ACL patch. Because of the assumptions made, it cannot fully describe the shear stress $\tau(y)$ in the viscoelastic layer. This can be seen by rewriting the expression for $\tau(y)$ given in Eq. (21) as

$$b \frac{L_a}{2} \tau(y) = f(y) \kappa_{\text{acl}}(e_p - e_b), \tag{40}$$

where $f(y)$ is a function describing the shape of $\tau(y)$ and is given by

$$f(y) = \frac{\zeta \sinh \sqrt{g}(y)}{\cosh(\zeta) - 1}. \tag{41}$$

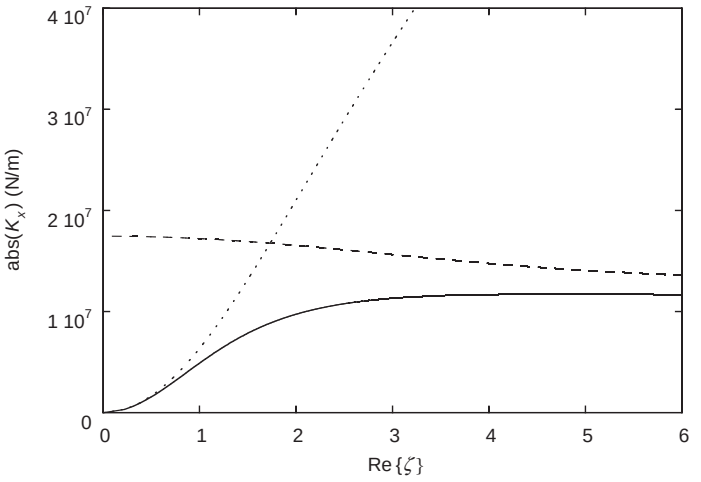

Fig. 9. Equivalent stiffness as a function of ζ: $\cdots$, κ_v; - - -, κ_c; ——, κ_{acl}.

Therefore, both the equivalent stiffness κ_{acl} and the shape function $f(y)$ are necessary to characterise the ACL patch. As a consequence, the loss factor of the ACL patch cannot be obtained directly from κ_{acl}, since the loss factor depends on the variation of $\tau(y)$ along the ACL patch (see Section 7 for the derivation of the loss factor).

5. The beam with ACL patch

In this section, we present the derivation of the lumped parameter model of a beam treated with an ACL patch. The classical modal decomposition method is applied to the equation of motion of the treated beam, using the modes of the untreated beam. In the resulting modal model, the ACL patch appears as a spring of stiffness K_{acl} coupled to a mass–spring system representing the base beam. The spring K_{acl} is made of two springs in series: one corresponds to the viscoelastic layer and has a complex stiffness K_v, the other corresponds to the cover layer and has a stiffness K_c which is approximately real.

5.1. Equation of motion of a beam treated with ACL

A beam is treated with an ACL patch on a portion of its length, as shown in Fig. 3. Since the mass and the bending stiffness of the ACL patch are neglected, the only effect of the patch is to apply a shear stress τ to the base beam. The equation of motion of the beam is

$$E_b I_b \frac{\mathrm{d}^4 W}{\mathrm{d}x^4} - \rho\omega^2 W = b\,\frac{t_b}{2}\,\frac{\mathrm{d}\tau}{\mathrm{d}x} + F_{\mathrm{ext}}\delta(x - x_e). \tag{42}$$

If the conditions for the strain to be constant underneath the ACL patch are fullfilled (Eqs. (10) and (11)), then the shear stress on the beam becomes, from Eq. (40),

$$\tau(x) = \frac{1}{b}\frac{2}{L_a} f(x)\kappa_{\text{acl}}(e_p - e_b)\Pi(x), \tag{43}$$

where

$$\Pi(x) = \begin{cases} 1 & \forall x \in [x_1, x_2], \\ 0 & \text{otherwise.} \end{cases} \tag{44}$$

It is worth noting that the model can easily account for multiple ACL treatments by simply summing the shear stresses from each patch. In Eq. (43), the extension e_b can be expressed as

$$e_b = u_{bv2} - u_{bv1} = -\frac{t_b}{2}\left(\frac{\mathrm{d}W}{\mathrm{d}x}(x_2) - \frac{\mathrm{d}W}{\mathrm{d}x}(x_1)\right). \tag{45}$$

Inserting Eqs. (43) and (45) in Eq. (42) yields

$$\begin{aligned} E_c I_c \frac{\mathrm{d}^4 W}{\mathrm{d}x^4} - \rho\omega^2 W - \frac{t_b^2}{2L_a}\kappa_{\text{acl}}\left(\frac{\mathrm{d}W}{\mathrm{d}x}(x_2) - \frac{\mathrm{d}W}{\mathrm{d}x}(x_1)\right)\frac{\mathrm{d}}{\mathrm{d}x}(f(x)\Pi(x)) \\ = \frac{t_b}{L_a}\kappa_{\text{acl}} e_p \frac{\mathrm{d}}{\mathrm{d}x}(f(x)\Pi(x)) + F_{\text{ext}}\delta(x - x_e). \end{aligned} \tag{46}$$

5.2. Modal decomposition

Following the classical modal decomposition approach, we assume the transversal deflection $W(x,\omega)$ is given by

$$W(x,\omega) = \sum_n W_n(\omega)\Phi_n(x), \tag{47}$$

where $W_n(\omega)$ and $\Phi_n(x)$ are the modal amplitude and the mode shape of the nth mode of the untreated beam, respectively. Inserting Eq. (47) into (46) yields

$$\begin{aligned} \sum_n \left[\Phi_n \rho(\omega_n^2 - \omega^2) W_n - \frac{t_b^2}{2L_a}\kappa_{\text{acl}}\Delta\Psi_n \frac{\mathrm{d}}{\mathrm{d}x}(f(x)\Pi(x))W_n\right] \\ = \frac{t_b}{L_a}\kappa_{\text{acl}} e_p \frac{\mathrm{d}}{\mathrm{d}x}(f(x)\Pi(x)) + F_{\text{ext}}\delta(x - x_e). \end{aligned} \tag{48}$$

In this equation,

$$\omega_n^2 = \frac{E_b I_b}{\rho} k_n^4 \tag{49}$$

is the nth natural frequency of the untreated beam and $\Delta\Psi_n = \Psi_n(x_2) - \Psi_n(x_1)$ where $\Psi_n(x) = \mathrm{d}\Phi_n(x)/\mathrm{d}x$.

We multiply Eq. (48) by $\Phi_m(x)$ and integrate over the length of the beam. Because of the orthogonality of the modes, we obtain

$$M_m(\omega_m^2 - \omega^2)W_m - \frac{t_b^2}{2L_a}\kappa_{\text{acl}}\sum_n \Gamma_m[\Delta\Psi_n W_n] = \frac{t_b}{L_a}\,\kappa_{\text{acl}} e_p \Gamma_m + F_m, \tag{50}$$

where

$$M_m = \int_0^L \rho\Phi_m(x)^2\,\mathrm{d}x \tag{51}$$

and

$$F_m = F_{\text{ext}}\Phi_m(x_e) \tag{52}$$

are the modal mass and the modal force of the mth mode and where

$$\Gamma_m = \int_0^L \Phi_m(x)\frac{\mathrm{d}}{\mathrm{d}x}(f(x)\Pi(x))\,\mathrm{d}x. \tag{53}$$

Integrating twice this last equation by parts yields

$$\Gamma_m = -[F(x)\Psi_n(x)\Pi(x)]_0^L + \int_{x_1}^{x_2} F(x)\frac{\mathrm{d}\Psi_n(x)}{\mathrm{d}x}\,\mathrm{d}x, \tag{54}$$

where $F(x)$ is the primitive of $f(x)$. Since the strain is assumed to be constant beneath the ACL patch, $\mathrm{d}\Psi_n/\mathrm{d}x$ is also constant between x_1 and x_2 (see Eq. (8)) and therefore

$$\Gamma_m = -b\frac{L_a}{2}\frac{\mathrm{d}\Psi_m(x_c)}{\mathrm{d}x}\frac{E_c t_c}{\kappa_c}. \tag{55}$$

The non-dimensional term Γ_m quantifies the coupling between the function $f(y)$ and the host beam at position x_c, and can therefore be referred to as a "position coupling factor". As expected, Γ_m is maximum when x_c is located on an antinode of the mth mode.

The terms Γ_m and $\Delta\Psi_n$ are not orthogonal, and mode-coupling effects appear in Eq. (50). This is because the ACL patch applies forces which couple the uncontrolled modes of the beam. These effects are now assumed to be negligible, i.e.

$$\Gamma_m\sum_n[\Delta\Psi_n W_n] \approx \Gamma_m\,\Delta\Psi_m\,W_m. \tag{56}$$

This results in

$$W_n\left[M_n(\omega_n^2 - \omega^2) - \frac{t_b^2}{2L_a}\,\kappa_{\text{acl}}\Delta\Psi_n\Gamma_n\right] = \frac{t_b}{L_a}\kappa_{\text{acl}}\Gamma_n e_p + F_n. \tag{57}$$

This equation can be rewritten as

$$W_n M_n(\omega_n^2 - \omega^2) = K_{\text{acl}}(e_p - a_n W_n) + F_n, \tag{58}$$

where

$$K_{\text{acl}} = \frac{t_b}{L_a}\,\Gamma_n\kappa_{\text{acl}} \tag{59}$$

and

$$a_n = -\frac{t_b}{2} L_a \frac{\mathrm{d}\Psi_n(x_c)}{\mathrm{d}x}. \tag{60}$$

Eq. (58) is the lumped parameter model of the beam treated with ACL, as shown in Fig. 10. The left-hand side of Eq. (58) describes a mass-spring system and corresponds to the nth mode of the host beam. The right-hand side of the equation describes a spring of modal stiffness K_{acl} and corresponds to the ACL patch, K_{acl} being the stiffness of the ACL patch seen by the host structure. This spring responds to the extension e_p induced in the actuator by the control voltage, and to the extension $e_b = a_n W_n$ of the host beam beneath the ACL patch. The non-dimensional term a_n corresponds to the coupling between the bending motion and the extensional motion beneath the ACL patch, and is represented in Fig. 10 by a lever between the mass–spring system and the base of the ACL spring. The spring K_{acl} is made of two springs in series, K_c and K_v, given by

$$K_c = \frac{t_b}{L_a} \Gamma_n \kappa_c \tag{61}$$

and

$$K_v = \frac{t_b}{L_a} \Gamma_n \kappa_v, \tag{62}$$

as discussed in the previous section. The real part of K_{acl} can be either positive or negative, depending on the sign of Γ_n. This sign, in its turn, depends on $\mathrm{d}\Phi_n(x_c)/\mathrm{d}x$, and thus on the position of the ACL patch on the beam. However, the real part of $a_n K_{\mathrm{acl}}$ is always positive, because a_n and K_{acl} always have the same sign.

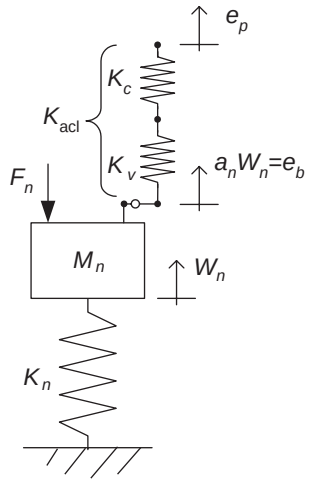

Fig. 10. sdof model of a beam treated with ACL.

6. Validation of the model

In this section, the lumped parameter model is numerically validated by comparing predictions with those obtained from a model based on the wave approach. This wave model has been experimentally validated by Illaire and Kropp [10] on a treated beam similar to the one considered in this section, showing very good agreement up to 2 kHz.

The structure we consider is a simply supported aluminium beam of dimensions $0.4 \times 0.03 \times 0.003\,\mathrm{m}^3$, onto which is bonded a massless ACL patch with the characteristics given in Table 1. The patch has a length of 5 cm, and is glued to the beam between the positions $x_1 = 0.25\,\mathrm{m}$ and $x_2 = 0.30\,\mathrm{m}$. These characteristics result in $|\zeta| = 1.5$, which corresponds to an optimal efficiency of the ACL patch, as will be discussed in Section 7. For the sake of simplicity, the shear modulus of the viscoelastic layer is assumed to be independent of frequency, and the loss factor is assumed to be zero in the cover layer and in the host beam.

The assumption of constant strain discussed in Section 3 requires the inequalities (10) and (11) to hold. Values for the first six modes of the beam considered in this section are listed in Table 2.

The beam is excited either by a force applied at the position $x = 0.25$, i.e. at the left end of the ACL patch, or with a voltage applied to the actuator of the patch. In both cases, the response of the structure is calculated by summing the responses of the first 12 modes.

As shown in Fig. 11, the frequency response function (FRF) calculated using the lumped parameter model agrees well with that calculated with the wave model which involves few assumptions. Agreement around antiresonances tends to appear worse, because in these frequency ranges the single-mode approximation is worse. These results are not surprising since the modification of the mass and stiffness of the base beam due to the ACL patch is negligible, and the primary effect of the ACL patch is to add damping to the structure. Therefore, when Eqs. (10) and (11) are not fulfilled for a certain mode, the overall aspect of the response remains correct and only the amplitude of this mode is not accurately predicted.

Table 1
ACL patch properties

	Thickness (m)	Storage modulus ($\mathrm{N\,m^{-2}}$)	Loss factor	Strain constant
Viscoelastic layer	0.127×10^{-3}	10.7×10^{6}	1	—
Cover layer	0.5×10^{-3}	62.1×10^{9}	0	120×10^{-12}

Table 2
Values taken by Eqs. (10) and (11) for the first six modes of the treated beam

	Mode 1	Mode 2	Mode 3	Mode 4	Mode 5	Mode 6
$\frac{L_a}{2}k_n\lvert\cot k_n x_c\rvert$	0.13	0.16	2.96	0.79	0.20	2.84
$\frac{1}{2}\left(\frac{L_a}{2}k_n\right)^2$	0.02	0.08	0.17	0.31	0.48	0.69

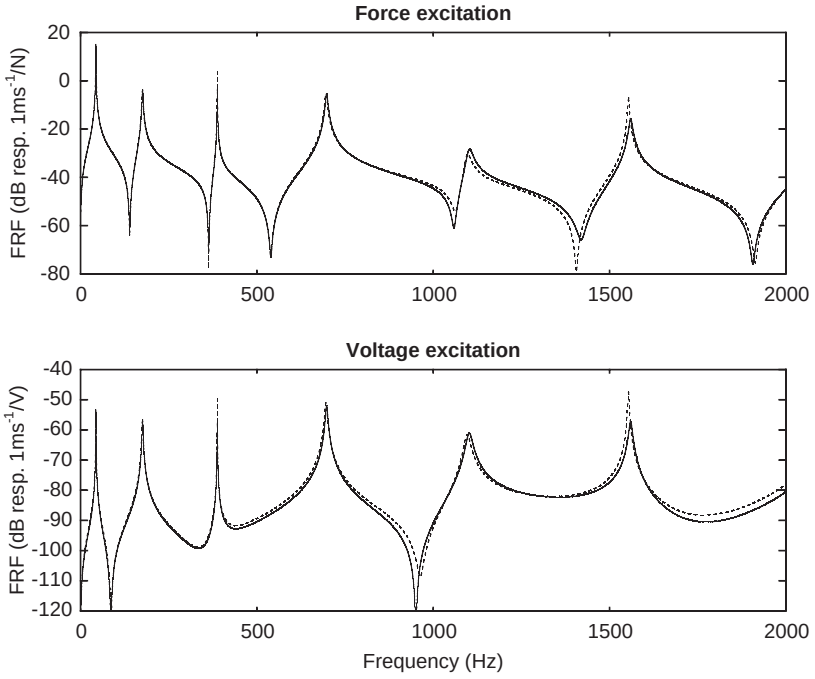

Fig. 11. FRF magnitude: wave model vs. modal model: ——, wave model; · · ·, modal model.

In order to investigate more closely the accuracy of the lumped parameter model, it is worth to compute the difference between the amplitudes of the resonance peaks predicted by the two models. Indeed, since damping in the base and cover layers is neglected, the amplitudes of the resonances depend only on the accuracy of the modelling of the damping in the viscoelastic layer. As can be seen in Fig. 12, the differences are small, except for modes 3 and 6 which are not well approximated using the constant strain assumption of Eqs. (10) and (11). In this case, the amplitude predicted by the lumped parameter model is overestimated, indicating that the damping is too low in this model.

7. The model: ACL damping discussion

In the previous sections, a simple lumped parameter model was developed and validated, which describes the behaviour of the host structure as an sdof system for frequencies around the nth resonance. In this section, the phenomena associated with ACL damping are discussed and described in terms of the parameters of this model, for a simply supported beam and at a single mode. The behaviour of the system is discussed for passive control (i.e. $V = 0$) and active control, where V is some function of W and its time derivative. For the sake of clarity, the subscript n is omitted henceforth. Eq. (58) is then rewritten as

$$M\ddot{W} + KW = F - K_{\mathrm{acl}} aW + K_{\mathrm{acl}} e_p. \tag{63}$$

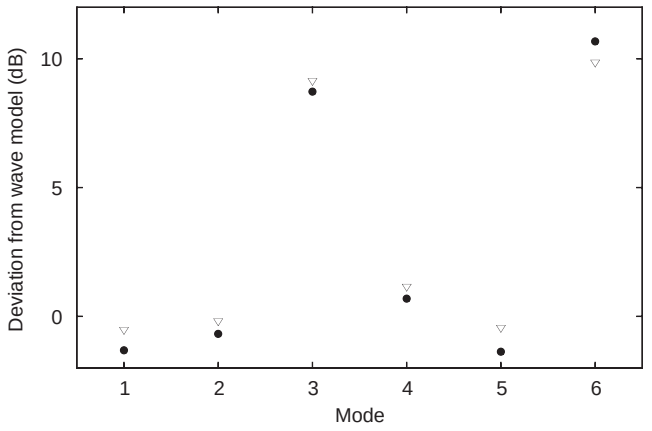

Fig. 12. Deviation of the amplitudes of the resonances. •, force excitation; ▽, voltage excitation.

7.1. Passive configuration

In the passive configuration, the extension e_p induced in the actuator by the control voltage is zero and hence the effect of the ACL patch is to add to the base beam a stiffness equal to aK_{acl}. With the assumptions made in this work, the real part of this stiffness is negligible in comparison with the stiffness K of the base beam. Therefore, the ACL patch in effect adds a loss factor η_p equal to

$$\eta_p = a\frac{\mathrm{Im}\{K_{\mathrm{acl}}\}}{\mathrm{Re}\{K\}}. \tag{64}$$

As expected, the loss factor depends on the coupling a between bending and extension beneath the ACL patch and on the imaginary part of the stiffness of the patch coupled to the beam. Since $K_{\mathrm{acl}} = t_b/L_a\Gamma_n\kappa_{\mathrm{acl}}$ (Eq. (59)), this imaginary part depends on the coupling factor Γ_n and on the imaginary part of the stiffness of the uncoupled ACL patch, $\mathrm{Im}\{\kappa_{\mathrm{acl}}\}$. When the storage modulus G' and the loss factor η_G of the viscoelastic material are constant with frequency, $\mathrm{Im}\{\kappa_{\mathrm{acl}}\}$ is maximum for $|\zeta|$ close to 1.5, which corresponds to a ratio $|\kappa_c/\kappa_v|$ also around 1.5. In practice, G' and η_G strongly vary with frequency, thus the optimum value of $|\zeta|$ might be different. In any case, it is possible to optimise the design of the ACL patch to maximise the passive damping.

Expressing η_p in terms of the physical parameters of the structure yields, for a simply supported beam,

$$\eta_p = 6\,\frac{L_a}{L}\,\frac{E_c}{E_b}\,\frac{t_c}{t_b}\sin^2 k_n x_c\,\frac{\mathrm{Im}\{\kappa_{\mathrm{acl}}\}}{\kappa_c}. \tag{65}$$

This equation highlights how η_p depends on the size and stiffness of the ACL patch compared to those of the host beam, on the position of the patch and on right design of the ACL patch. This equation also shows that, except for the term $\sin^2 k_n x_c$ which describes the coupling between the

patch and the beam at position x_c, η_p does not depend on the mode number and thus on the frequency. This is because in the model it is assumed that the length of the patch is much smaller than the length of the host structure.

7.2. Active configuration

In the case of an active treatment, W obeys

$$W(K - M\omega^2) = F + K_{\text{acl}}(e_p - aW). \tag{66}$$

This equation shows that the material damping increases if e_p, and thus the control voltage, is in phase with $-W$. In this case the extension applied to the spring K_{acl}, and thus the dissipation of energy in this spring, is augmented. If e_p is equal to αW, where α is a real constant, then

$$W = \frac{F}{K + K_{\text{acl}}(a - \alpha) - M\omega^2}. \tag{67}$$

The total loss factor η is therefore given by

$$\eta = (a - \alpha)\,\frac{\text{Im}\{K_{\text{acl}}\}}{K + (a - \alpha)\text{Re}\{K_{\text{acl}}\}}. \tag{68}$$

When the active stiffness due to the control voltage can be neglected compared to the stiffness K of the base beam, then

$$\eta = \eta_p + \eta_a, \tag{69}$$

where η_a is the loss factor due to the augmented material damping, and is given by

$$\eta_a = -\frac{\alpha}{a}\,\eta_p. \tag{70}$$

In order to increase the total loss factor, α should be either positive or negative, depending on the sign of a, i.e. on the location of the ACL patch on the beam. Since the sign of a might be different for different modes, η_a might be negative at certain frequencies if α is constant over a broad frequency range. It is therefore necessary to sense the strain of the surface of the beam beneath the ACL patch, in order to insure that the control voltage increases the shearing motion of the viscoelastic layer. This might be done using, e.g. an accelerometer, a piezofilm sensor or the self-sensing actuator technique developed by Dosh et al. [11]. Note that in theory, η_a is infinite for infinite values of α, but in practice the amplitude of the control voltage is limited.

Another way of controlling the vibrations is to apply active forces to the host structure through the viscoelastic layer, as can be seen by rewriting Eq. (66) as

$$W(K - M\omega^2 + K_{\text{acl}}) = F + F_a, \tag{71}$$

where F_a is the active force and is equal to

$$F_a = K_{\text{acl}} e_p. \tag{72}$$

If e_p is equal to $-\beta\dot{W}$ (where β is a real constant), the actuator of the ACL patch behaves as an active viscous damper. In this case, the response of the beam at resonance is equal to

$$W = \frac{F}{\mathrm{Im}\{K_{\mathrm{acl}}(a + \mathrm{j}\beta)\}} = \frac{F}{a\,\mathrm{Re}\{K_{\mathrm{acl}}\}\eta_p + \beta\,\mathrm{Re}\{K_{\mathrm{acl}}\}}. \tag{73}$$

An interesting case arises when $F + F_a = 0$, i.e. when

$$e_p = L_a \frac{d_{31}}{t_c} V = -\frac{F}{K_{\mathrm{acl}}}. \tag{74}$$

In this case, the total input power into the structure is zero and so is the response. In practice, complete cancellation cannot be achieved. Eq. (74) shows that the control voltage optimising the active forces effect is finite, and decreases as K_{acl} increases. This result suggests that K_{acl} should be chosen as high as possible, i.e. the actuator should be bonded directly to the beam; however, this choice would result in a low amount of material damping in the structure, and the beneficial effects of material damping on the stability of the control as well as on the fail-safe characteristics of the treatment would be lost; there is therefore a compromise. Eq. (74) also shows that the optimal control voltage is in phase with $-F$. In cases where feedforward control is possible, this phase relationship might be easy to implement, and will usually strongly depend on frequency. In other cases, since at resonance the force is in phase with the velocity of the beam, the active control is essentially a derivative feedforward control. This type of control becomes less efficient away from the resonance, but of course control is of less importance there. An additional beneficial effect of having material damping in the structure is therefore to increase the efficiency of the effect of the active actions in the case of feedback control.

These results are consistent with those of Gandhi and Munski [12] who, using a finite element formulation on a beam treated with ACL, found that the effects of increasing material damping are dominant when proportional feedback control is used, while the control due to transmission of active forces to the host structure is dominant when derivative feedback is used.

8. Conclusion

This paper described a simple model of beams treated with ACL, which provides insight into the physics of ACL treatments. In this model, each mode of the base beam is modelled as an sdof system, and the two layers of the ACL patch are modelled by two springs in series. The spring representing the viscoelastic layer has a complex stiffness, and the spring modelling the actuator is driven by the control voltage applied to the piezoelectric layer. Since the main assumption of the model is that the longitudinal displacement of the beam beneath the ACL patch varies linearly with position, the model is valid for patches whose length is short compared to the wavelength on the beam and which are positioned at appropriate locations on the beam.

The strength of the model lies in its simplicity, since it enables analytical investigation of the effects of the parameters of the ACL patch and of the control voltage on the efficiency of the

different ACL damping mechanisms. Furthermore, the viscoelastic layer can be chosen arbitrarily thin and stiff, thus enabling piezoelectric patches directly bonded to the host structure to be modelled. Additionally, multiple patch treatments can easily be modelled by connecting several springs to the base beam model. A numerical validation showed that, despite its simplicity, the model accurately predicts the response of beams treated with ACL patches.

The various mechanisms of ACL control were briefly discussed for a single mode. In the passive case, it was shown that the efficiency of the ACL patch depends on the product of a term describing the coupling of the ACL patch with the beam at the position where the patch is centred, and of the imaginary part of the uncoupled patch. In the active case, the control voltage increases the material damping (i.e. the dissipation of energy in the viscoelastic layer) and/or apply active forces to the beam through the viscoelastic layer.

Material damping augmentation occurs when the control voltage is proportional to the displacement of the beam and as large as possible. To ensure maximum efficiency of this damping mechanism, the passive material damping should be optimised.

Active forces effects are optimum when the control voltage is proportional to the external force applied to the beam. At resonances, this occurs when the control voltage is proportional to the velocity of the beam (derivative feedback). In this case, the active forces also introduce active viscous damping in the structure. The amplitude of the control voltage cancelling the external force has to be determined and decreases when the coupling between the ACL patch and the beam increases. To minimise the amplitude of the control voltage, the viscoelastic layer should thus be chosen as stiff as possible. However, this design would decrease the amount of material damping in the structure, and thus the stability of the control. There is therefore a compromise.

The model was proved useful to understand the physics of ACL treatments, and will be used in future work to optimise the design of these treatments, as well as to compare the conventional ACL configuration to treatments consisting of a passive constrained layer and an actuator separately bonded to the beam.

References

[1] A. Baz, J. Ro, Performance characteristics of active constrained layer damping, *Proceedings of the SPIE, The International Society for Optical Engineering* 2193 (1994) 98–114.

[2] W.H. Liao, K.W. Wang, Characteristics of enhanced active constrained layer damping treatments with edge elements—Part i: finite element model development and validation, *Journal of Vibration and Acoustics* 120 (4) (1998) 886–893.

[3] C.H. Park, A. Baz, Vibration control of bending modes of plates using active constrained layer damping, *Journal of Sound and Vibration* 227 (4) (1999) 711–734.

[4] J.A. Rongong, J.R. Wright, R.J. Wynne, G.R. Tomlinson, Modelling of a hybrid constrained layer/piezoceramic approach to active damping, *Journal of Vibration and Acoustics* 119 (1) (1997) 120–130.

[5] A. Baz, Active constrained layer damping, in: *Damping'93 Conference*, vol. 3, San Francisco, CA, 1993, pp. IBB 1–23.

[6] A. Baz, J. Ro, Partial treatment of flexible beams with active constrained layer damping, in: *Conference of Engineering Science Society*, vol. ASME-AMD 67, Charlottesville, VA, 1993, pp. 61–80.

[7] A. Baz, Boundary control of beams using active constrained layer damping, *Journal of Vibration and Acoustics* 119 (2) (1997) 166–172.

[8] I.Y. Shen, Hybrid damping through intelligent constrained layer treatments, *Journal of Vibration and Acoustics* 116 (3) (1994) 341–349.
[9] I.Y. Shen, A variational formulation, a work–energy relation and damping mechanisms of active constrained layer treatments, *Journal of Vibration and Acoustics* 119 (2) (1997) 192–199.
[10] H. Illaire, W. Kropp, Quantification of damping mechanisms of active constrained layer treatments, *Journal of Sound and Vibration* 281 (1–2) (2005) 189–217; doi:10.1016/j.jsv.2004.01.032.
[11] J. Dosh, D.J. Inman, E. Garcia, A self-sensing piezoelectric actuator for collocated control, *Journal of Intelligent Material Systems and Structures* 3 (1992) 166–185.
[12] F. Gandhi, B.E. Munsky, Comparison of the mechanism and effectiveness of position and velocity feedback in active constrained-layer damping treatments, *Proceedings of the SPIE, The International Society for Optical Engineering* 3989 (2000) 61–72.